

---

# SHINE: Sequential Hierarchical Integration Network for EEG and MEG

---

Anonymous Author(s)

Affiliation  
Address  
email

## Abstract

How natural speech is represented in the brain constitutes a major challenge for cognitive neuroscience, with cortical envelope-following responses playing a central role in speech decoding. This paper presents our approach to the Speech Detection task in the LibriBrain Competition 2025, utilizing over 50 hours of magnetoencephalography (MEG) signals from a single participant listening to LibriVox audiobooks. We introduce the proposed Sequential Hierarchical Integration Network for EEG and MEG (SHINE) to reconstruct the binary speech-silence sequences from MEG signals. In the Extended Track, we further incorporated auxiliary reconstructions of speech envelopes and Mel spectrograms to enhance training. Ensemble methods combining SHINE with baselines (BrainMagic, AWavNet, ConvConcatNet) achieved F1-macro scores of 0.9155 (Standard Track) and 0.9184 (Extended Track) on the leaderboard test set.

## 1 Introduction

How natural speech is represented in the brain remains a major challenge in cognitive neuroscience. Over the past two decades, neuroscientists have made seminal contributions, progressively elucidating the pivotal role of cortical envelope-following responses—wherein the auditory cortex tracks the amplitude modulations of acoustic signals (1; 2). These responses constitute a foundational neural mechanism for speech decoding, namely, the extraction of perceived speech from neural signals. In recent years, the rapid advancement of machine learning techniques has spurred some researchers aimed at decoding speech features (such as temporal envelopes and Mel spectrograms) from non-invasive neural recordings, such as magnetoencephalography (MEG) (3) and electroencephalography (EEG)(4).

This year, the Parker Jones Neural Processing Lab (PNPL) at the University of Oxford hosted the LibriBrain Competition 2025 (5). The organizers sourced stimuli from LibriVox, presented them to a single participant, and acquired over 50 hours of MEG data (6). Within the competition’s **Speech Detection** task, participants were tasked with training a model to **distinguish speech vs. silence** based on brain activity measured by MEG during a listening session. This challenge task comprises two tracks: the Standard Track permits the use of only the LibriBrain training dataset, whereas the Extended Track allows incorporation of any external data.

In this task, our team developed several innovative strategies as follows:

**1. Task Reformulation:** We restructured the conventional binary classification framework into a sequence reconstruction task, focusing on reconstructing a binary sequence directly from MEG signals. This reformulation more effectively captures the temporal dynamics of the MEG signals.

34 2. **SHINE model:** We proposed SHINE (Sequential Hierarchical Integration Network for EEG and  
35 MEG), an advanced neural architecture originally developed for reconstructing speech envelopes and  
36 Mel spectrograms from EEG signals.

37 3. **Multi-Feature Reconstruction Strategy (only in Extended Track):** To augment model training,  
38 we incorporated the reconstruction of speech envelopes and Mel spectrograms as auxiliary tasks  
39 alongside the primary binary sequence reconstruction during the training stage.

## 40 2 Methods

### 41 2.1 Datasets

42 The LibriBrain dataset (6) used for the competition contained non-invasive MEG recordings acquired  
43 from one healthy participant listening to over 50 hours of audiobooks, all sourced from LibriVox.  
44 The MEG recordings were acquired from 306 sensors covering the whole brain. Neural data were  
45 minimally filtered (e.g., to remove line noise and drift) and downsampled to 250 Hz. The data  
46 were standardly split into train, validation, and test sets. Though this standard split, all data were  
47 permissible for model training during the competition. For the competition, the organizer reserved an  
48 additional competition **holdout** split, which included disjoint subsets of data to be used to update the  
49 leaderboard during the competition and to decide the final ranking of submissions.

### 50 2.2 Task Reformulation

51 In the speech detection task, we needed to train a model to distinguish speech vs. silence based on  
52 brain activity measured by MEG during a listening session. The baseline routine provided by the  
53 organizers employed 0.8-second epochs of MEG data to predict the label at the central sampling  
54 point—designating it as speech (label 1) or silence (label 0). However, given the critical role of  
55 contextual information in speech decoding (7), we posited that decoding should leverage longer  
56 neural signal segments to better encapsulate temporal dependencies. This approach aligned with  
57 established sequence-to-sequence (seq2seq) paradigms in EEG-based speech decoding, such as the  
58 reconstruction of speech envelopes (8) or Mel spectrograms (9; 10; 11; 4).

59 Specifically, we adopted a comparable strategy, utilizing 30-second epochs of MEG signals to  
60 reconstruct a 30-second binary sequence, wherein 0 denoted silence and 1 denoted speech. To  
61 optimize this process, we employed the negative Pearson correlation coefficient as the loss function,  
62 enhancing the model’s ability to capture temporal dynamics effectively.

63 Speech perception involves hierarchical processing in the brain, with MEG signals reflecting neural  
64 responses to various levels of speech features (12). We hypothesized that these features could help to  
65 finish the binary sequence reconstruction task. To this end, we incorporated auxiliary reconstructions  
66 of the speech envelope and Mel spectrograms in the **Extended Track** to facilitate learning of the  
67 primary binary sequence. During the training stage, the envelope, a 10-sub-band Mel spectrograms,  
68 and the ground-truth binary sequence were concatenated along the sub-band dimension to form a  
69 composite 12-sub-band representation. In the validation stage, only the binary sequence was reserved  
70 to calculate the Pearson correlation coefficient with the target binary sequence.

### 71 2.3 Model

72 A Sequential **Hierarchical Integration Network for EEG and MEG** (SHINE), drawing inspiration from  
73 previous works (8; 4), was developed for the binary sequence reconstruction task. In this framework,  
74 the input comprised 30-second MEG signals, while the output is a binary sequence (speech: 1 and  
75 silence: 0). The architecture of SHINE consisted of six stacked blocks (Figure 1a, with each block  
76 encompassing four distinct components (Figure 1b,. Preceding these six blocks, two linear layers  
77 were employed to extract initial features, thereby compressing the MEG dimensionality from 306  
78 channels to 64. Subsequently, following the blocks, a convolutional neural network (CNN) and a long  
79 short-term memory (LSTM) module were integrated to derive higher-order global sequence features.

80 The first part of each block was the CNN stack consisting of 5 convolutional layers. The second part  
81 was a simple fully connected linear layer. The third part was the output context layer consisting of  
82 a zero-padding, a temporal convolutional layer, LeakyReLU activation function, and layer normal-  
83 ization. The last part was a self-attention layer. As shown in Figure 1c, each of the first four layers

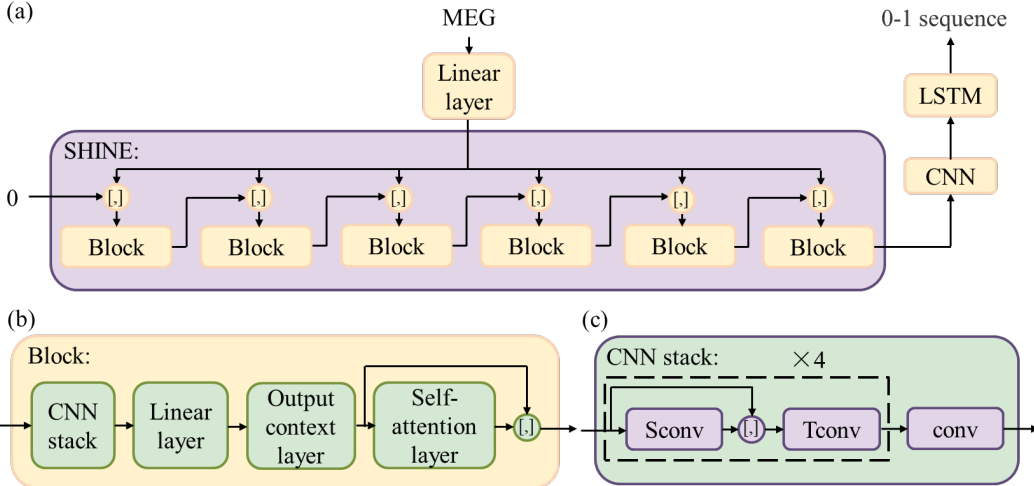


Figure 1: Structure of the proposed SHINE. (a) the overall network architecture of SHINE. (b) four different parts in each block. (c) the network architecture of the CNN stack.

84 in the CNN stack contains Sconv and Tconv. Sconv was a pointwise convolution followed by LLP  
 85 (Layer normalization, LeakyReLU activation function, and zero-padding). Tconv was a temporal  
 86 convolution with groups equal to the input channel number followed by LLP. The last layer in the  
 87 CNN stack, conv, contained a simple temporal convolutional layer followed by LLP.

88 The architecture extensively leveraged concatenation operations to facilitate the hierarchical integration  
 89 of speech-relevant information embedded within MEG signals. As shown in Figures 1a and 1b,  
 90 the MEG after the initial linear layer, the output of the output context layer, and the output of the  
 91 self-attention layer were concatenated along the channel dimension and used as the input for the next  
 92 block. Additionally, in the CNN stack, the output of Sconv was concatenated with the initial input  
 93 along the channel dimension.

#### 94 2.4 Training and Validation

95 We combined the officially split training and validation sets to enable subsequent cross-validation  
 96 analyses. This integrated corpus comprised over 50 hours of MEG recordings spanning 92 distinct  
 97 sessions. Considering temporal autocorrelations (TAs) (13) prevalent in MEG signals within indi-  
 98 vidual sessions, which might undermine the model's ability to discern speech-relevant features, we  
 99 adopted a "leave-session-out" splitting to mitigate overfitting to session-specific TAs features (14; 15).  
 100 In each training iteration, 8 sessions were randomly selected from the 92 to constitute the validation  
 101 set, with the remainder allocated to training.

102 The neural networks were implemented with PyTorch and trained on an NVIDIA A800 GPU.  
 103 Optimization was performed via the AdamW algorithm to maximize predictive correlation, with  
 104 an initial learning rate of  $10^{-3}$  and a weight decay coefficient of 0.01. Training was capped at a  
 105 maximum of 20 epochs. The loss function comprised the negative Pearson correlation coefficient  
 106 between predicted and ground-truth sequences.

#### 107 2.5 Testing

108 We designated the officially split test dataset as the "**Local test**", while the subset reserved for  
 109 leaderboard updates upon submission was termed the "**leaderboard test**". Performance metrics  
 110 for our used models were reported across both datasets. The pilot experiment revealed declined  
 111 reconstruction performance at the start and the end of the reconstructed sequence. Accordingly, we  
 112 discarded the initial and terminal 5-second segments from seq2seq outputs prior to evaluation. The  
 113 metric used in the task was the F1-macro score, details in Section A.1.

114 **2.6 Baseline Models and Ensemble**

115 To enhance model performance, we implemented an ensemble learning framework. Within this  
116 ensemble, in addition to the proposed SHINE model, we incorporated several established models for  
117 EEG signal reconstruction, including ConvConcatNet (4), AWavNet (16), and BrainMagic (3). We  
118 hypothesized that their inclusion would augment the ensemble's diversity, thereby improving overall  
119 robustness.

120 Throughout the course of the competition, we iteratively refined the hyperparameters and random  
121 seeds of the SHINE, as well as those baseline models. Ultimately, for each track, we archived over  
122 200 trained models to enable the final ensemble.

123 **3 Results**

124 We compared the performance of SHINE with baseline models. Each model underwent hyperparameter  
125 fine-tuning to optimize the F1-macro score. Table 1 delineated the highest scores attained by each  
126 model on the leaderboard test set.

Table 1: F1-macro score on the Local test and Leaderboard test for the Standard and Extended Track

Model	Standard Track		Extended Track	
	Local test	Leaderboard test	Local test	Leaderboard test
BrainMagic	0.8996	0.8912	0.8999	0.8951
AWavNet	0.8974	0.8881	0.8993	0.8905
ConvConcatNet	0.8988	0.8917	0.9007	0.8956
SHINE	<b>0.9067</b>	<b>0.9015</b>	<b>0.9097</b>	<b>0.9045</b>

127 For the Extended Track, we augmented each model by concurrently reconstructing Mel spectrograms  
128 and speech envelopes during the training stage. These results demonstrated that such auxiliary  
129 training strategy enhanced overall model efficacy.

130 Finally, we ensembled over 200 models by refining the hyperparameters and random seeds of four  
131 mentioned models for each track. This integrative approach yielded macro-averaged F1 scores  
132 (F1-macro) of **0.9155** in the Standard Track and **0.9184** in the Extended Track.

133 **4 Discussion**

134 The proposed SHINE network achieves efficient extraction of MEG features through iterative con-  
135 catenation, with its core architecture predicated on CNN. Prior research posits that CNN functions  
136 analogously to matched filters, thereby enabling the capture of signal "templates" from low signal-  
137 to-noise ratio EEG and MEG signals (17). This property may underpin one of the key factors  
138 contributing to the SHINE network's commendable performance in the present competition, further  
139 underscoring the important role of CNNs in neural signal decoding (18; 19; 20; 21; 22; 23).

140 In recent EEG decoding works, architectures such as Transformers (24; 25) and Mamba (26) have  
141 been used to improve performance. However, constrained by the time limit in this competition, our  
142 similar explorations failed to yield performance gains. Such avenues nonetheless hold promise as  
143 prospective directions for future enhancements.

144 **5 Conclusion**

145 In this work, we proposed a novel SHINE model for reconstructing binary speech-silence sequences  
146 from MEG signals, demonstrating superior performance in the LibriBrain Competition 2025. Through  
147 task reformulation into a seq2seq framework, integration of auxiliary speech features in the Extended  
148 Track, and ensemble learning with diverse baselines, our approach achieved high F1-macro scores,  
149 underscoring the importance of capturing temporal dynamics and hierarchical neural processing in  
150 speech detection. Future work should explore architectures like Transformers or Mamba to achieve  
151 better results.

152 **References**

- 153 [1] E. Ahissar, S. Nagarajan, M. Ahissar, A. Protopapas, H. Mahncke, and M. M. Merzenich,  
154 “Speech comprehension is correlated with temporal response patterns recorded from auditory  
155 cortex,” *Proceedings of the National Academy of Sciences*, vol. 98, no. 23, pp. 13 367–13 372,  
156 2001.
- 157 [2] H. Luo and D. Poeppel, “Phase patterns of neuronal responses reliably discriminate speech in  
158 human auditory cortex,” *Neuron*, vol. 54, no. 6, pp. 1001–1010, 2007.
- 159 [3] A. Défossez, C. Caucheteux, J. Rapin, O. Kabeli, and J.-R. King, “Decoding speech perception  
160 from non-invasive brain recordings,” *Nature Machine Intelligence*, vol. 5, no. 10, pp. 1097–1107,  
161 2023.
- 162 [4] X. Xu, B. Wang, Y. Yan, H. Zhu, Z. Zhang, X. Wu, and J. Chen, “ConvConcatNet: A deep  
163 convolutional neural network to reconstruct mel spectrogram from the EEG,” in *2024 IEEE  
164 International Conference on Acoustics, Speech, and Signal Processing Workshops (ICASSPW)*,  
165 2024, pp. 113–114.
- 166 [5] G. Landau, M. Özdogan, G. Elvers, F. Mantegna, P. Somaiya, D. Jayalath, L. Kurth, T. Kwon,  
167 B. Shillingford, G. Farquhar, M. Jiang, K. Jerbi, H. Abdelhedi, Y. Mantilla Ramos, C. Gulcehre,  
168 M. Woolrich, N. Voets, and O. P. Jones, “The 2025 PNPL competition: Speech detection and  
169 phoneme classification in the libribrain dataset,” no. arXiv:2506.10165, 2025, arXiv:2506.10165  
170 [cs].
- 171 [6] M. Özdogan, G. Landau, G. Elvers, D. Jayalath, P. Somaiya, F. Mantegna, M. Woolrich, and  
172 O. P. Jones, “LibriBrain: Over 50 hours of within-subject MEG to improve speech decoding  
173 methods at scale,” no. arXiv:2506.02098, 2025, arXiv:2506.02098 [cs].
- 174 [7] D. A. Moses, S. L. Metzger, J. R. Liu, G. K. Anumanchipalli, J. G. Makin, P. F. Sun, J. Chartier,  
175 M. E. Dougherty, P. M. Liu, G. M. Abrams, A. Tu-Chan, K. Ganguly, and E. F. Chang,  
176 “Neuroprosthesis for decoding speech in a paralyzed person with anarthria,” *New England  
177 Journal of Medicine*, vol. 385, no. 3, pp. 217–227, 2021.
- 178 [8] B. Accou, J. Vanthornhout, H. Van Hamme, and T. Francart, “Decoding of the speech envelope  
179 from EEG using the VLAAI deep neural network,” *Scientific Reports*, vol. 13, no. 11, p. 812,  
180 2023.
- 181 [9] L. Bollens, C. Puffay, B. Accou, J. Vanthornhout, H. Van Hamme, and T. Francart, “Auditory  
182 EEG decoding challenge for ICASSP 2024,” *IEEE Open Journal of Signal Processing*, pp.  
183 1–12, 2025.
- 184 [10] C. Fan, S. Zhang, J. Zhang, E. Liu, X. Li, G. Zhao, and Z. Lv, “DMF2Mel: A dynamic  
185 multiscale fusion network for EEG-driven mel spectrogram reconstruction,” in *Proceedings of  
186 the 33rd ACM International Conference on Multimedia*, ser. MM ’25, New York, NY, USA,  
187 2025, pp. 6977–6985.
- 188 [11] C. Fan, S. Zhang, J. Zhang, Z. Pan, and Z. Lv, “SSM2Mel: State space model to reconstruct  
189 mel spectrogram from the EEG,” in *ICASSP 2025 - 2025 IEEE International Conference on  
190 Acoustics, Speech and Signal Processing (ICASSP)*, 2025, pp. 1–5.
- 191 [12] B. Wang, X. Xu, Z. Zhang, H. Zhu, Y. Yan, X. Wu, and J. Chen, “Self-supervised speech  
192 representation and contextual text embedding for match-mismatch classification with EEG  
193 recording,” in *2024 IEEE International Conference on Acoustics, Speech, and Signal Processing  
194 Workshops (ICASSPW)*, 2024, pp. 111–112.
- 195 [13] X. Xu, B. Wang, B. Xiao, Y. Niu, Y. Wang, X. Wu, H. Cheng, and J. Chen, “The impacts of  
196 temporal autocorrelations on EEG decoding,” *Biomedical Signal Processing and Control*, vol.  
197 113, p. 108783, 2026.
- 198 [14] C. Puffay, B. Accou, L. Bollens, M. Jalilpour Monesi, J. Vanthornhout, H. Van Hamme, and  
199 T. Francart, “Relating EEG to continuous speech using deep neural networks: a review,” *Journal  
200 of Neural Engineering*, vol. 20, no. 4, p. 041003, 2023.

- 201 [15] I. Rotaru, S. Geirnaert, N. Heintz, I. Van de Ryck, A. Bertrand, and T. Francart, “What are  
202 we really decoding? unveiling biases in EEG-based decoding of the spatial focus of auditory  
203 attention,” *Journal of Neural Engineering*, vol. 21, no. 1, p. 016017, 2024.
- 204 [16] Y. Fang, H. Li, X. Zhang, F. Chen, and G. Gao, “Cross-attention-guided wavenet for mel  
205 spectrogram reconstruction in the ICASSP 2024 auditory EEG challenge,” in *2024 IEEE  
206 International Conference on Acoustics, Speech, and Signal Processing Workshops (ICASSPW)*,  
207 2024, pp. 7–8.
- 208 [17] L. Stanković and D. Mandić, “Convolutional neural networks demystified: A matched filtering  
209 perspective-based tutorial,” *IEEE Transactions on Systems, Man, and Cybernetics: Systems*,  
210 vol. 53, no. 6, pp. 3614–3628, 2023.
- 211 [18] B. Accou, M. Jalilpour Monesi, J. Montoya, H. Van hamme, and T. Francart, “Modeling the  
212 relationship between acoustic stimulus and EEG with a dilated convolutional neural network,”  
213 in *2020 28th European Signal Processing Conference (EUSIPCO)*, 2021, pp. 1175–1179.
- 214 [19] Z. Qiu, J. Gu, D. Yao, and J. Li, “Exploring auditory attention decoding using speaker features,”  
215 in *INTERSPEECH 2023*, 2023, pp. 5172–5176.
- 216 [20] Z. Qiu, J. Gu, D. Yao, J. Li, and Y. Yan, “BMMSNet: Bidirectional mapping and multilevel  
217 similarity comparison for EEG-speech match-mismatch problem,” in *2024 IEEE International  
218 Conference on Acoustics, Speech, and Signal Processing Workshops (ICASSPW)*, 2024, pp.  
219 117–118.
- 220 [21] Z. Qiu, D. Yao, and J. Li, “StreamAAD: Decoding spatial auditory attention with a streaming  
221 architecture,” in *2024 IEEE 14th International Symposium on Chinese Spoken Language  
222 Processing (ISCSLP)*, 2024, pp. 1–5.
- 223 [22] S. Vandecappelle, L. Deckers, N. Das, A. H. Ansari, A. Bertrand, and T. Francart, “EEG-based  
224 detection of the locus of auditory attention with convolutional neural networks,” *eLife*, vol. 10,  
225 p. e56481, 2021.
- 226 [23] X. Xu, B. Wang, Y. Yan, X. Wu, and J. Chen, “A DenseNet-based method for decoding auditory  
227 spatial attention with EEG,” in *International Conference on Acoustics, Speech and Signal  
228 Processing (ICASSP)*, Piscataway, 2024, pp. 1946–1950.
- 229 [24] L. Bollens, B. Accou, H. Van hamme, and T. Francart, “Contrastive representation learning with  
230 transformers for robust auditory EEG decoding,” *Scientific Reports*, vol. 15, no. 1, p. 28744,  
231 2025.
- 232 [25] Q. Ni, H. Zhang, C. Fan, S. Pei, C. Zhou, and Z. Lv, “DBPNet: Dual-branch parallel network  
233 with temporal-frequency fusion for auditory attention detection,” in *Proceedings of the Thirty-  
234 Third International Joint Conference on Artificial Intelligence (IJCAI)*, 2024, pp. 1–9.
- 235 [26] C. Fan, H. Zhang, Q. Ni, J. Zhang, J. Tao, J. Zhou, J. Yi, Z. Lv, and X. Wu, “Seeing helps  
236 hearing: A multi-modal dataset and a mamba-based dual branch parallel network for auditory  
237 attention decoding,” *Information Fusion*, p. 102946, 2025.

238 **A Appendix**

239 **A.1 Evaluation Criteria**

$$F1_{macro} = \frac{1}{K} \sum_{k=1}^K 2 \cdot \frac{\text{Precision}_k \cdot \text{Recall}_k}{\text{Precision}_k + \text{Recall}_k} \quad (1)$$

240 This is the unweighted average of per-class F1 scores, where the F1 score is the harmonic mean of  
241 Precision and Recall. Here, each class k is speech or silence for Speech Detection. For reference,  
242 Precision and Recall can be defined in terms of True Positives (TP), False Positives (FP), and False  
243 Negatives (FN), each of which is an integer count:

$$\text{Precision} = \frac{\text{TP}}{\text{TP} + \text{FP}}, \quad \text{Recall} = \frac{\text{TP}}{\text{TP} + \text{FN}}, \quad F1 = \frac{2 \cdot \text{TP}}{2 \cdot \text{TP} + \text{FP} + \text{FN}} \quad (2)$$